REPORT NO. DOT-TSC-OST-76-13

STUDY OF AERODYNAMIC DRAG REDUCTION ON A FULL-SCALE TRACTOR-TRAILER

L.L. Steers
L.C. Montoya

NATIONAL AERONAUTICS AND SPACE ADMINISTRATION
DRYDEN FLIGHT RESEARCH CENTER
PO Box 273
Edwards CA 93523

APRIL 1976
FINAL REPORT

Prepared for
U.S. DEPARTMENT OF TRANSPORTATION
OFFICE OF THE SECRETARY
Office of the Assistant Secretary
for Systems Development and Technology
Office of Systems Engineering
Washington DC 20590

NOTICE

This document is disseminated under the sponsorship of the Department of Transportation in the interest of information exchange. The United States Government assumes no liability for its contents or use thereof.

NOTICE

The United States Government does not endorse products or manufacturers. Trade or manufacturers' names appear herein solely because they are considered essential to the object of this report.

Technical Report Documentation Page

1. Report No.	2. Government Accession No.	3. Recipient's Catalog No.
DOT-TSC-OST-76-13		

4. Title and Subtitle	5. Report Date
STUDY OF AERODYNAMIC DRAG REDUCTION ON A FULL-SCALE TRACTOR-TRAILER	April 1976
	6. Performing Organization Code
7. Author(s)	8. Performing Organization Report No.
L. L. Steers and L. C. Montoya	DOT-TSC-OST-76-13
9. Performing Organization Name and Address	10. Work Unit No. (TRAIS)
NASA Dryden Flight Research Center* P. O. Box 273 Edwards CA 93523	OS614/R6506
	11. Contract or Grant No.
	RA-74-31
12. Sponsoring Agency Name and Address	13. Type of Report and Period Covered
U.S. Department of Transportation and National Aeronautics Office of the Secretary and Space Administration Office of the Assistant Secretary Washington DC 20546 for Systems Development and Technology Office of Systems Engineering Washington DC 20590	Final Report March to December 1974
	14. Sponsoring Agency Code

15. Supplementary Notes

*Under a Reimbursable Agreement with: U.S. Department of Transportation
Transportation Systems Center
Kendall Square
Cambridge MA 02142

16. Abstract

Aerodynamic drag tests were performed on a tractor-trailer combination using the coast-down method on a smooth, nearly level runway. The tests included an investigation of drag reduction obtained with add-on devices that are commercially available or under development. The tests covered tractor-trailer speeds ranging from approximately 35 to 65 miles per hour and included fuel consumption measurements. The study shows the effects of the various add-on devices on the aerodynamic drag, and for some devices on the fuel consumption. Results from a simulation of fuel consumption tests using a computer program are also included.

17. Key Words	18. Distribution Statement
Aerodynamic Drag Tractor-Trailer Add-On Devices Fuel Economy	DOCUMENT IS AVAILABLE TO THE U.S. PUBLIC THROUGH THE NATIONAL TECHNICAL INFORMATION SERVICE, SPRINGFIELD, VIRGINIA 22161

19. Security Classif. (of this report)	20. Security Classif. (of this page)	21. No. of Pages	22. Price
Unclassified	Unclassified	58	

Form DOT F 1700.7 (8-72) Reproduction of completed page authorized

PREFACE

This report presents the results of a joint National Aeronautics and Space Administration-Department of Transportation study of the aerodynamic drag of a full-scale tractor-trailer combination. Tests included determining the effects on aerodynamic drag of five different drag-reduction add-on devices that are commercially available or under development. A basic tractor-trailer combination and a tractor-trailer combination fitted with an add-on device were used to test the effects of variation in aerodynamic drag on fuel consumption. The results of computer simulations for fuel consumption are also included. The full-scale fuel consumption tests reported herein show fuel savings of up to about 10 percent, depending on wind conditions and the device employed.

METRIC CONVERSION FACTORS

Approximate Conversions to Metric Measures

Symbol	When You Know	Multiply by	To Find	Symbol
		LENGTH		
in	inches	2.5	centimeters	cm
ft	feet	30	centimeters	cm
yd	yards	0.9	meters	m
mi	miles	1.6	kilometers	km
		AREA		
in^2	square inches	6.5	square centimeters	cm^2
ft^2	square feet	0.09	square meters	m^2
yd^2	square yards	0.8	square meters	m^2
mi^2	square miles	2.6	square kilometers	km^2
	acres	0.4	hectares	ha
		MASS (weight)		
oz	ounces	28	grams	g
lb	pounds	0.45	kilograms	kg
	short tons (2000 lb)	0.9	tonnes	t
		VOLUME		
tsp	teaspoons	5	milliliters	ml
Tbsp	tablespoons	15	milliliters	ml
fl oz	fluid ounces	30	milliliters	ml
c	cups	0.24	liters	l
pt	pints	0.47	liters	l
qt	quarts	0.95	liters	l
gal	gallons	3.8	liters	l
ft^3	cubic feet	0.03	cubic meters	m^3
yd^3	cubic yards	0.76	cubic meters	m^3
		TEMPERATURE (exact)		
°F	Fahrenheit temperature	5/9 (after subtracting 32)	Celsius temperature	°C

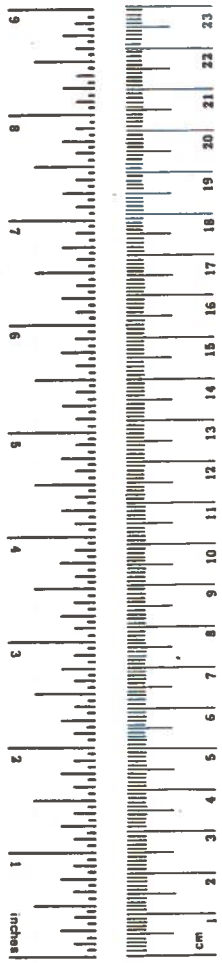

Approximate Conversions from Metric Measures

Symbol	When You Know	Multiply by	To Find	Symbol
		LENGTH		
mm	millimeters	0.04	inches	in
cm	centimeters	0.4	inches	in
m	meters	3.3	feet	ft
m	meters	1.1	yards	yd
km	kilometers	0.6	miles	mi
		AREA		
cm^2	square centimeters	0.16	square inches	in^2
m^2	square meters	1.2	square yards	yd^2
km^2	square kilometers	0.4	square miles	mi^2
ha	hectares (10,000 m^2)	2.5	acres	
		MASS (weight)		
g	grams	0.035	ounces	oz
kg	kilograms	2.2	pounds	lb
t	tonnes (1000 kg)	1.1	short tons	
		VOLUME		
ml	milliliters	0.03	fluid ounces	fl oz
l	liters	2.1	pints	pt
l	liters	1.06	quarts	qt
l	liters	0.26	gallons	gal
m^3	cubic meters	35	cubic feet	ft^3
m^3	cubic meters	1.3	cubic yards	yd^3
		TEMPERATURE (exact)		
°C	Celsius temperature	9/5 (then add 32)	Fahrenheit temperature	°F

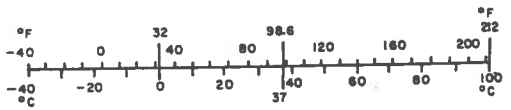

TABLE OF CONTENTS

LIST OF FIGURES

LIST OF FIGURES (CONTINUED)

LIST OF TABLES

LIST OF SYMBOLS AND ABBREVIATIONS

a	acceleration
A	frontal cross-sectional area (does not include the under-carriage and tires), 94 square feet
$C_{D_{ae}}$	aerodynamic drag coefficient, $\frac{D_{ae}}{qA}$
D	drag
F	resisting force
g	local acceleration of gravity
h	height
mpg	miles per gallon
mph	miles per hour
q	dynamic pressure, $0.5\ \rho V^2$
R	rotational thrust
V	velocity
w	width
W	vehicle weight during each test
x	distance between back of cab and front of trailer, 40 inches or 62 inches
Z_1	rolling resistance coefficient (0.00675)
Z_2	rolling resistance coefficient (0.000074)
$\Delta C_{D_{ae}}$	change in aerodynamic drag coefficient
Δt	time increment
ΔV	velocity increment
ρ	air density

Subscripts:

ae	aerodynamic
m	mechanical
t	total
tr	tractive

1. SUMMARY

The effects of five add-on devices on reducing the aerodynamic drag of a full-scale tractor trailer were examined experimentally using the coast-down technique. Over-the-road fuel consumption testing was conducted with the two add-on devices which provided the greatest reduction in aerodynamic drag. In addition, computer simulations were performed to establish the applicability of the simulation technique to evaluate improvements in tractor-trailer aerodynamics. The major findings of this study are summarized below:

1. The maximum fuel savings realized were approximately 10 percent for the most effective drag reduction devices when tested under calm wind conditions.

2. Aerodynamic drag reductions realized from the add-on devices under consideration ranged from a maximum of approximately 24 percent down to a minimum of 3 percent, under conditions of zero wind and with the trailer at its rear-most position (cab-to-trailer gap of 62 inches).

3. The ability of some of the devices to decrease drag was reduced under crosswind conditions.

4. Computer simulations of the fuel economy improvement of the aerodynamically improved tractor-trailer agreed closely with full-scale road test results.

5. Moving the trailer forward from its rear-most position (cab-to-trailer gap of 62 inches) to its forward-most position (cab-to-trailer gap of 40 inches) reduced the aerodynamic drag for the baseline configuration approximately 10 percent.

2. INTRODUCTION

Because of the recent fuel oil crisis, the conservation of fuel oil products has become a matter of greater concern to everyone. The resulting high prices and sometimes limited quantities of gasoline and diesel fuel have caused increased interest in ground vehicle efficiency. In the past, when ground vehicle fuel was comparatively inexpensive and readily available, the aerodynamic drag (wind resistance) of some high-volume carriers during design was considered unimportant. The high aerodynamic drag of these designs (i.e., box shapes) was merely overcome by more powerful engines, with resulting increases in fuel consumption.

In the fall of 1973, in response to the fuel crisis and increased interest in the aerodynamic drag of ground vehicles, the NASA Hugh L. Dryden Flight Research Center began a drag reduction program on a representative box-shaped ground vehicle (refs. 1 and 2). After baseline data were obtained for the vehicle with all square corners, the vehicle was modified by rounding the corners and sealing the undercarriage. The resulting reduction in aerodynamic drag exceeded 50 percent, which is equivalent to a fuel savings of approximately 15 percent to 25 percent at highway speeds.

In the wake of these results, the Department of Transportation and the National Aeronautics and Space Administration initiated the subject program, reported herein, in the spring of 1974. Initial results of this joint effort have been reported (refs. 3 and 4). The goal of the program was to assess the performance gains on a tractor-trailer combination provided by the addition of several different types of low-cost drag-reduction devices. These add-on devices, which are commercially available, or potentially available, were developed by private business concerns to reduce the aerodynamic drag of existing tractor-trailer combinations with only minor modifications.

A representative cab-over-engine tractor-trailer combination without any devices attached (the basic vehicle) was tested first. The tests were then repeated with the add-on devices installed. This report presents an evaluation of the drag reduction results

obtained with each of five add-on devices using the coast-down technique and the results of the fuel economy tests with two of the add-on devices.

The Department of Transportation's Power and Propulsion Branch of the Mechanical Engineering Division of the Transportation Systems Center (TSC) performed vehicle computer simulations to establish the fuel economy sensitivity of tractor-trailers to aerodynamic drag. The baseline vehicle has been analytically constructed with similar characteristics (weight, engine, transmission, etc.) as the tractor-trailer used for the actual vehicle tests presented in this report. Results of simulations using four different drag coefficients and two vehicle weights are presented.

3. TEST VEHICLE

The tractor-trailer combination test vehicle (fig. 1) consisted of a cab-over-engine tractor and a 45-foot-long, two-axle, smooth-sidewall trailer. The front vertical corners of the trailer had a 12-inch radius. The total gross weight of the test vehicle was approximately 32,000 pounds. General specifications of the test vehicle are given in table 1.

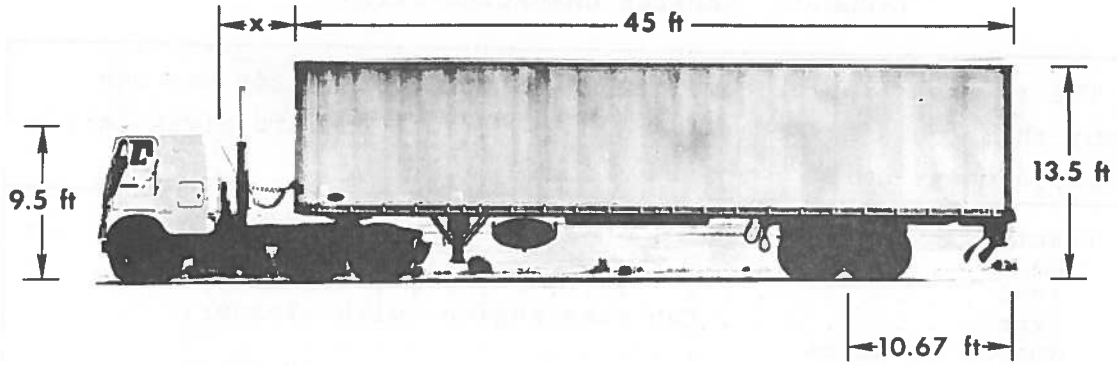

SIDE VIEW

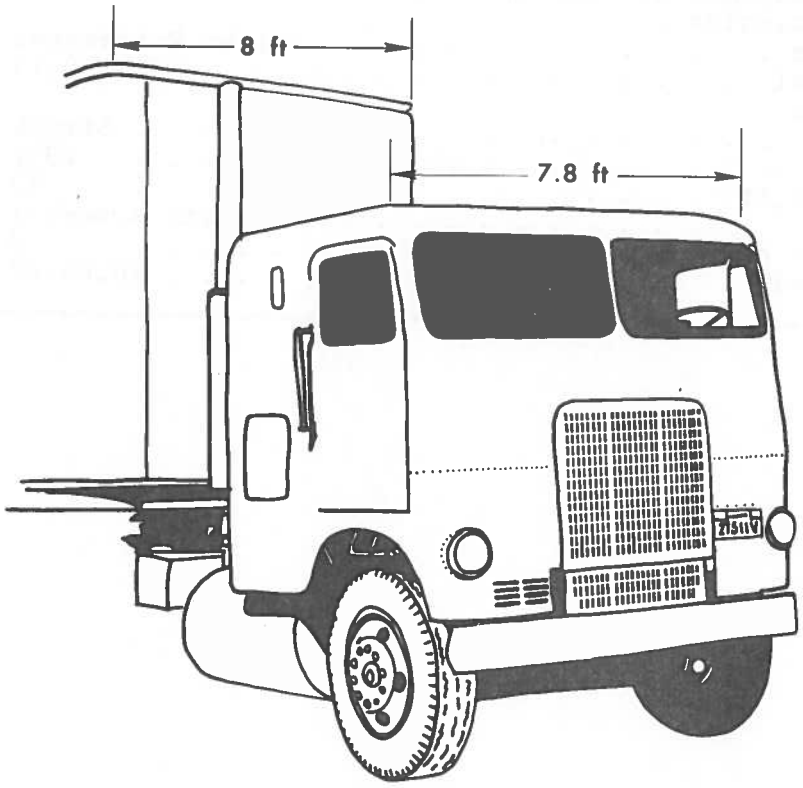

THREE-QUARTER FRONT VIEW

FIGURE 1. TEST VEHICLE

TABLE 1. VEHICLE CHARACTERISTICS

The tractor-trailer combination used in this study was one of many that could have been used. Specifications are given herein for completeness only.

Tractor:	
Make	White Freightliner
Year	1974
Type	Cab over engine (with sleeper)
Number of axles	3
Tire size	10.00-22
Engine-	
Type	350 Cummings Turbocharged
Model	NTC-350
Displacement, in^3	855
Horsepower at 2100 rpm	310
Transmission-	
Type	Fuller Roadranger
Model	RTO-9513
Trailer:	
Make	Strick
Year	1972
Length, ft	45
Type	Smooth sidewall
Number of axles	2
Tire size	10.00-22

4. METHOD

4.1 TOTAL DRAG

For this study, total drag is considered to be the retarding force that can be directly derived from the deceleration of the coasting vehicle. The components of the total drag and its definition are as follows:

$$D_t = D_m + D_{ae} = \frac{\Delta V}{\Delta t}\frac{W}{g} \qquad (1)$$

where the total drag is the sum of the mechanical drag (D_m) and aerodynamic drag (D_{ae}). By setting the manual transmission in neutral during each deceleration run, the mechanical drag consisted of: (1) the tractive drag of the tires and bearings and the gear resistance back through the drive line to the transmission; and (2) the thrust from the rotational inertia of the wheels and tires. The coast-down method as used for these tests has been applied under very carefully controlled conditions. Tire pressure was kept nearly constant by filling the tires with nitrogen, which reduces temperature effects. Vehicle weight was determined for each day of testing and was not permitted to vary significantly to keep mechanical or rolling drag as constant as possible between tests. By keeping mechanical drag constant, any changes in drag resulting from the addition of the devices would be aerodynamic in origin.

The test vehicle was accelerated to a few miles per hour above the starting velocity of each test, and the manual transmission was then disengaged. The time it took for the truck to decelerate to given speeds was recorded and used to calculate total drag values from the above-stated definition. A more complex approach to the coast-down method is decribed in reference 5.

Two methods of employing the coast-down technique were used. In the first method an accelerometer was used to determine the vehicle's deceleration. In the second method, a precision speedometer (driven by a trailing "fifth wheel") and stopwatches were used for this purpose.

A small quanitity of drag data was obtained by using drive-shaft torque measurements. Drag was determined from the measured drive shaft torque and calculated drive shaft rotational velocity for constant velocity runs.

4.2 FUEL ECONOMY

The fuel consumption tests were performed by using two similar tractor-trailer combinations running simultaneously over a 300-mile course. The vehicles followed each other at a distance sufficient to prevent the trailing vehicle from being affected by the wake of the first.

Coast-down drag runs were first made with both vehicles to make sure that the total drag was the same for each. Then baseline fuel consumption runs were made with both vehicles to determine any differences in performance due to engine condition or tuning. Finally, one test vehicle was fitted with an add-on device. Two devices were tested in this way. Both tractors began each test with the fuel tanks topped off. The post-run fueling was delayed until the following morning so that the temperature of the fuel and the supply tanks would be the same. The tractors and supply tanks were routinely housed in the same environment to eliminate temperature differences. All top-off operations were done with the tractors parked on the same level floor.

The amount of fuel required to top off the fuel tank in each tractor was determined by weight, which was corrected for temperature effects.

4.3 SIMULATION STUDY*

For the computer simulation the baseline vehicle was assigned an aerodynamic drag coefficient equal to unity and vehicle simulations were performed for 20, 24, and 40 percent reductions in drag coefficient, and a 20 percent increase in drag coefficient. Two vehicle weights were considered: 32,500 pounds which is close to

*Simulations performed by E. Withjack, U.S. Department of Transportation, Transportation Systems Center, Cambridge MA.

the weight of the full-scale test vehicle and at 70,000 pounds to represent a fully-loaded vehicle. The above noted drag coefficient range encompasses typical values representative of tractor-trailer combinations.

The dynamics of the vehicle simulation model are based on Newton's second law. The force exerted by the drive wheels must overcome resisting forces due to aerodynamic drag, rolling resistance, acceleration, and road grade; this relationship is expressed by:

$$F_{wheel} = F_{ae} + F_{roll} + F_a + F_{grade} \quad (2)$$

With the grade force F_{grade} set equal to zero the remaining forces are determined from the following:

$$F_{ae} = q \times A \times C_{D_{ae}} \quad (3)$$

$$F_{roll} = W(Z_1 + Z_2 \times V) \quad (4)$$

$$F_a = \frac{aW}{g} \quad (5)$$

The torque at the driving wheels is determined using equation (2) and algebraically adding the appropriate rotating inertia. Values of speed and torque are analytically traced from the driving wheels through the propshaft and transmission to arrive at the torque input to the transmission. The engine is burdened by the transmission input torque, front end rotating inertias, and accessory load.

Engine torque and speed values are obtained from an engine map to obtain brake specific fuel consumption (lb/hp-hr). Typically, the engine map contains 14 load points and 10 speed points. Intermediate values of load and speed are obtained by appropriate linear interpolations.

More detailed information about the mechanics of the computer program can be found in reference 6.

5. TEST CONDITIONS

5.1 TOTAL DRAG

The coast-down drag tests were conducted on an Edwards Air Force Base runway, which had a concrete surface with a constant elevation gradient of 0.125 percent. The effect of this small gradient was eliminated by averaging successive runs in opposite directions. The tests covered vehicle speeds ranging from approximately 30 to 65 miles per hour. The vast majority of tests were made in calm wind conditions.

Tests were performed with a gap (x) of either 62 inches or 40 inches between the front of the trailer and the back of the top part of the cab (fig. 1).

During the first tests, it was found that the position of the thermostatically controlled radiator cooling shutters had a considerable and usually nonrepeatable effect on the drag measurements. To eliminate this variable, a cover that prevented airflow through the shutters was put over the radiator opening before each run (fig. 2).

5.2 FUEL CONSUMPTION

The fuel consumption tests were performed on the open highway. The route was approximately 300 miles long (fig. 3) and consisted primarily of open road with no severe grades. The twelfth gear was used most of the time because of the relatively light payloads of the vehicles. The vehicles followed each other at a distance sufficient to prevent the trailing vehicle from being affected by the wake of the first. Thus, both vehicles encountered the same environment.

Each of the two add-on devices used during the fuel consumption tests was evaluated over the course three times. In addition, three check runs were made with both tractor-trailer combinations in the baseline configuration. Two of these runs were made at the beginning of the fuel consumption study, and the third baseline check run was made after the add-on device runs were finished.

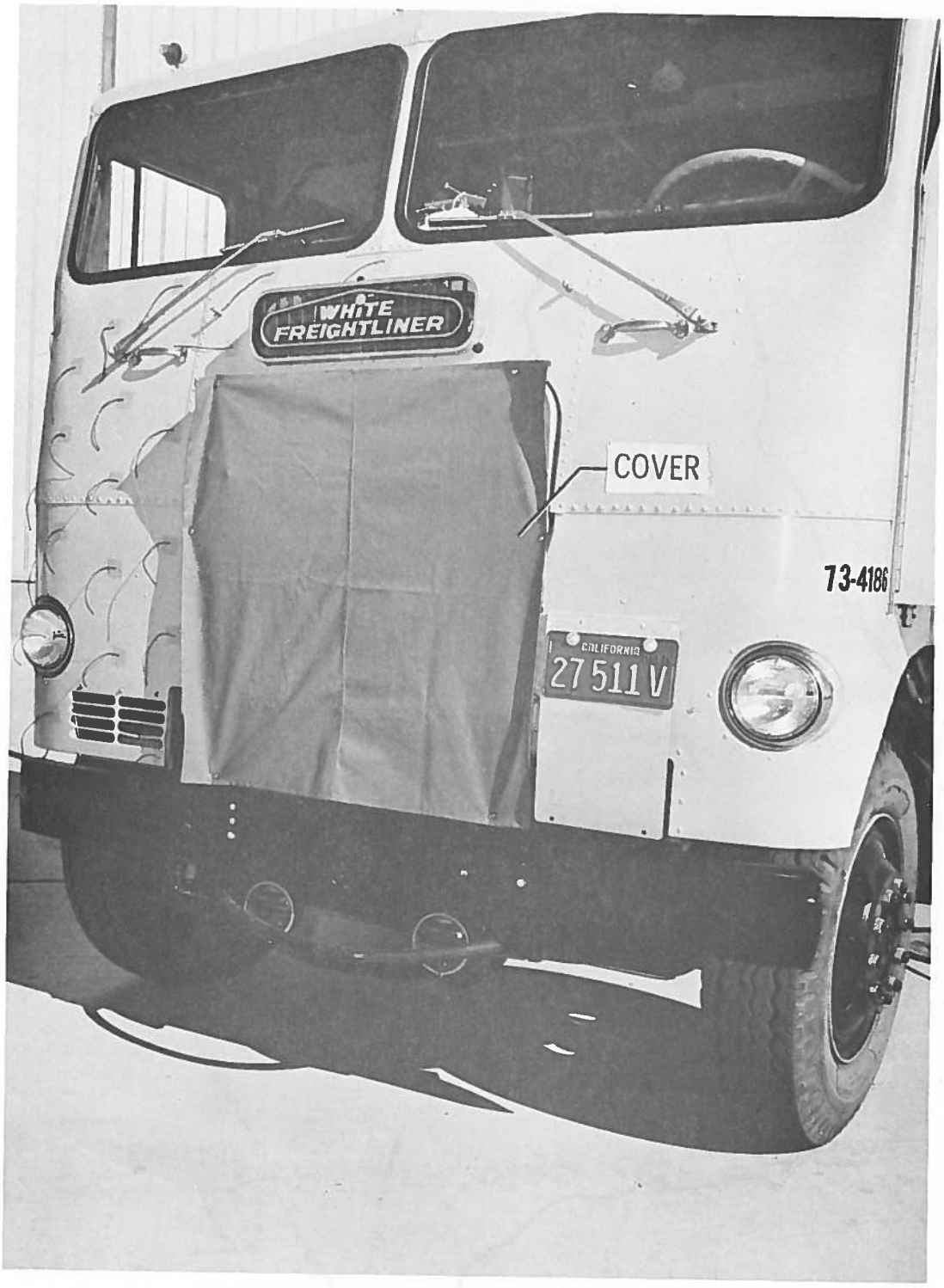

FIGURE 2. COVER OVER RADIATOR OPENING

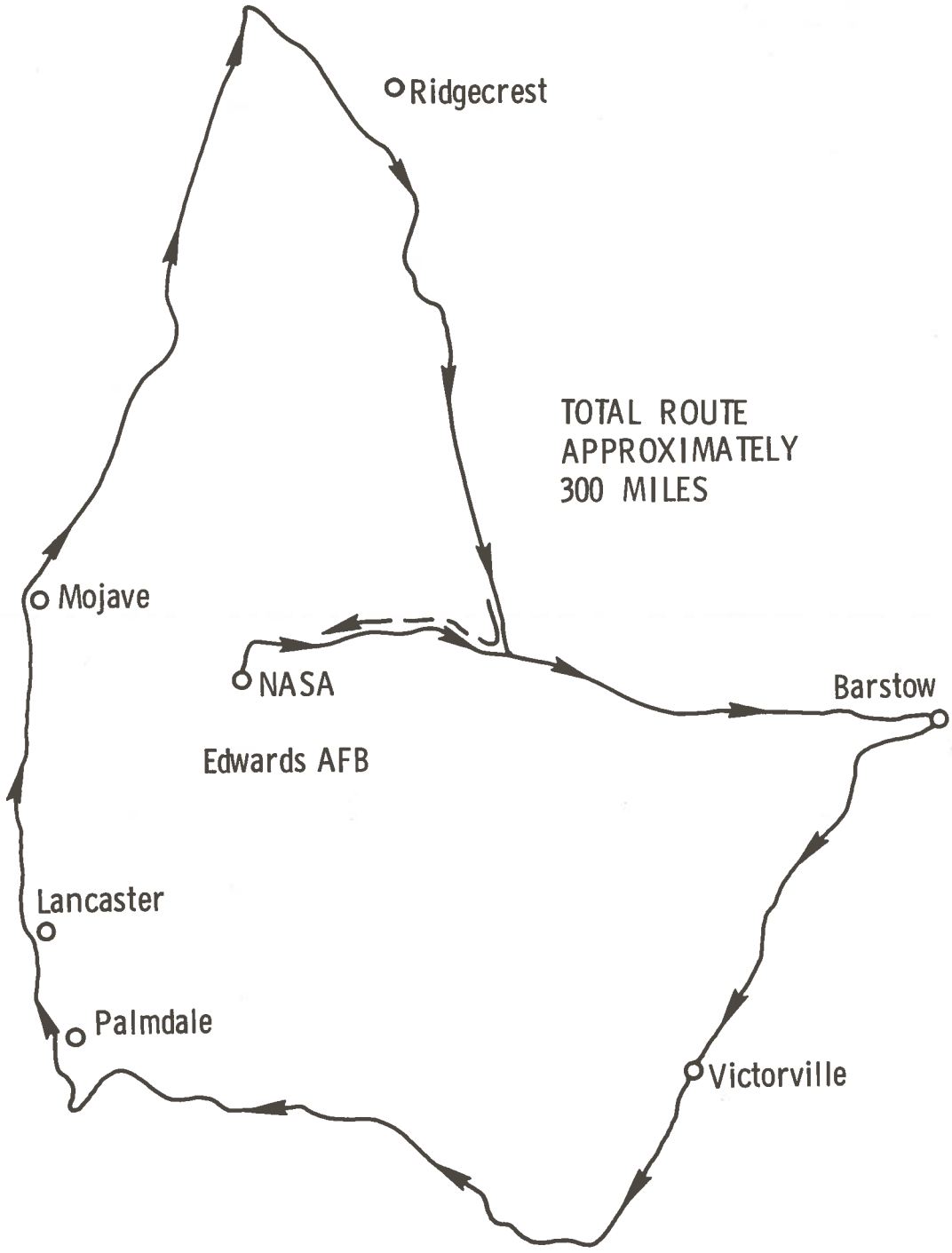

FIGURE 3. ROUTE FOR FUEL-CONSUMPTION TESTS

All the fuel consumption tests were performed with a 62-inch gap between the cab and trailer and at an average speed of 55 miles per hour.

During the aerodynamic drag tests and fuel consumption tests, histories of ambient pressure, temperature, wind velocity, and wind direction were recorded at Edwards AFB. General weather conditions during the fuel consumption tests were also noted in a qualitative way along the route, but no measurements were made.

6. INSTRUMENTATION

6.1 TOTAL DRAG

A ±0.1g accelerometer with 0.001g resolution was used to measure deceleration along with a bank of five 0.1-second stopwatches and a calibrated precision speedometer with a 0.1-mile-per-hour readout capability. The speedometer was driven by a fifth wheel. The velocity and distance of the fifth wheel was displayed digitally inside the truck's cab (fig. 4) along with the bank of stopwatches. The time increments corresponding to preselected velocity intervals in miles per hour (i.e., 60 to 55, 55 to 50, 50 to 45, 45 to 40, and 40 to 35) were obtained by starting all the stopwatches simultaneously at the starting test velocity and stopping them individually at the end of the desired velocity interval. A strain gage bridge on the tractor's drive shaft was used to measure the torque. The stopwatch data were hand recorded. The accelerometer, strain gage outputs and fifth wheel velocity outputs were recorded on tape and identified with an event marker during each test.

6.2 FUEL CONSUMPTION

Mileage for the fuel consumption runs was obtained from the calibrated tractor and trailer odometers. Radio communications were maintained between the vehicles so that the crews could coordinate shifting, engine start and stop times, and rpm. The radios were also used to coordinate the opening and closing of windows, vents, air conditioners, and fans during all the fuel consumption tests.

FIGURE 4. INSTRUMENTATION LAYOUT INSIDE CAB

7. DEVICES TESTED

The five add-on devices which were tested are shown as the cross-hatched areas in figure 5.

Device A, which was cab mounted, was 67 inches wide and 32 inches high. Device B, also cab mounted, was 52 inches wide and 27 inches high, with a 6.5-inch gap between the device and cab. Device C was trailer mounted and extended a maximum of 24 inches forward of the trailer. Device D was mounted at the top front edge of the trailer, with a 6-inch gap between the front edge of the device and trailer. Device E was 60 inches wide, cab mounted, and extended vertically 48 inches above the cab in the stored position and 38 inches above the cab in the fully deployed position, which is shown in figure 5. The deployment and storage of device E were automatic and depended on the impact pressure and its variation with velocity. Data for this device were acquired only for the fully deployed position and the rear trailer location (62-in. gap).

The three cab-mounted devices (devices A, B, and E) were designed to deflect more of the flow over the trailer. It appears that device C was designed to make the air flow smoothly around the trailer, and apparently device D was designed to maintain attached flow over the top of the trailer.

The manufacturers chose the device of the best size and proportions available at the time of purchase for the test vehicle. All the devices were installed according to manufacturer's instructions. The test results reported herein, therefore, are for the specific devices described above, mounted on the NASA test vehicle. A list of the manufacturers is included in the Appendix.

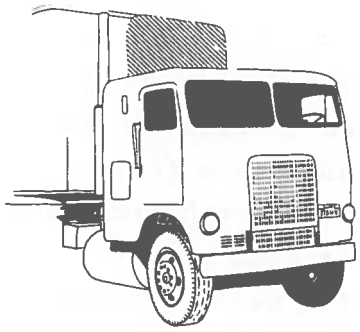

DEVICE A

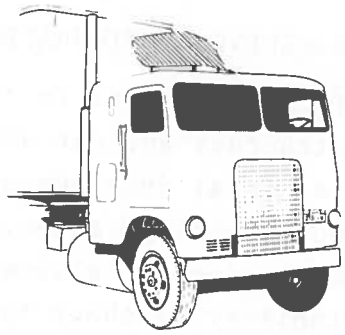

DEVICE B

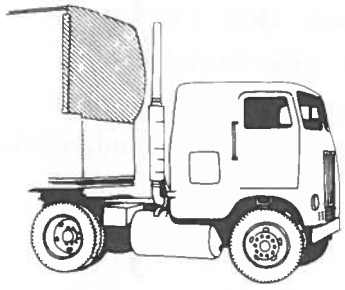

DEVICE C

DEVICE D

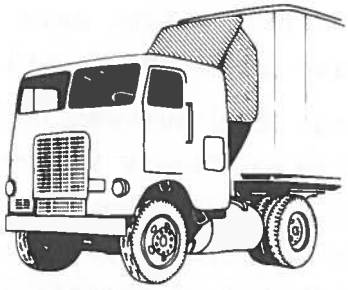

DEVICE E

FIGURE 5. DEVICES TESTED

8. RESULTS

8.1 BASELINE CONFIGURATION

Typical results for the baseline configuration from several stopwatch runs and one accelerometer run are shown in figure 6 in terms of total drag versus truck velocity. The data show that the two methods of measuring deceleration (i.e., stopwatch precision speedometer and accelerometer) are consistent with each other. Repeatability is shown by the stopwatch data, which were obtained on separate days by two different people. Total drag results obtained from a separate configuration equipped with a driveshaft torque device (other than baseline or A to E) are shown in figure 7. The results from all three methods tend to agree; however, the torque experience shown is limited.

Baseline data for the two trailer positions (gaps of 62-in. and 40-in.) are presented in figure 8. It is apparent that the total drag was lower when the distance between the cab and trailer was shorter. At 55 miles per hour, the total drag was reduced approximately 7 percent, which is equivalent to a reduction in aerodynamic drag of approximately 10 percent.

8.2 MODIFIED CONFIGURATIONS

The total drag with the various add-on devices installed is shown in figures 9 through 13. In figures 9 through 12 the cross-hatched region represents the drag range for the baseline vehicle; the lower bound is for the 40-inch gap and the upper bound is for the 62-inch gap. In figure 13 baseline data for only the 62-inch gap was shown because device E was tested only with a 62-inch gap.

The difference in total drag between the modified and baseline configurations is summarized in figure 14 for the two trailer positions at a speed of 55 miles per hour. As shown, the total drag reduction ranged from 18 percent for device A for the rear trailer position to approximately 2 percent for device D for both trailer positions. (The letters A, B, C. D, and E were assigned to the devices according to the chronological testing sequence and not according to rank).

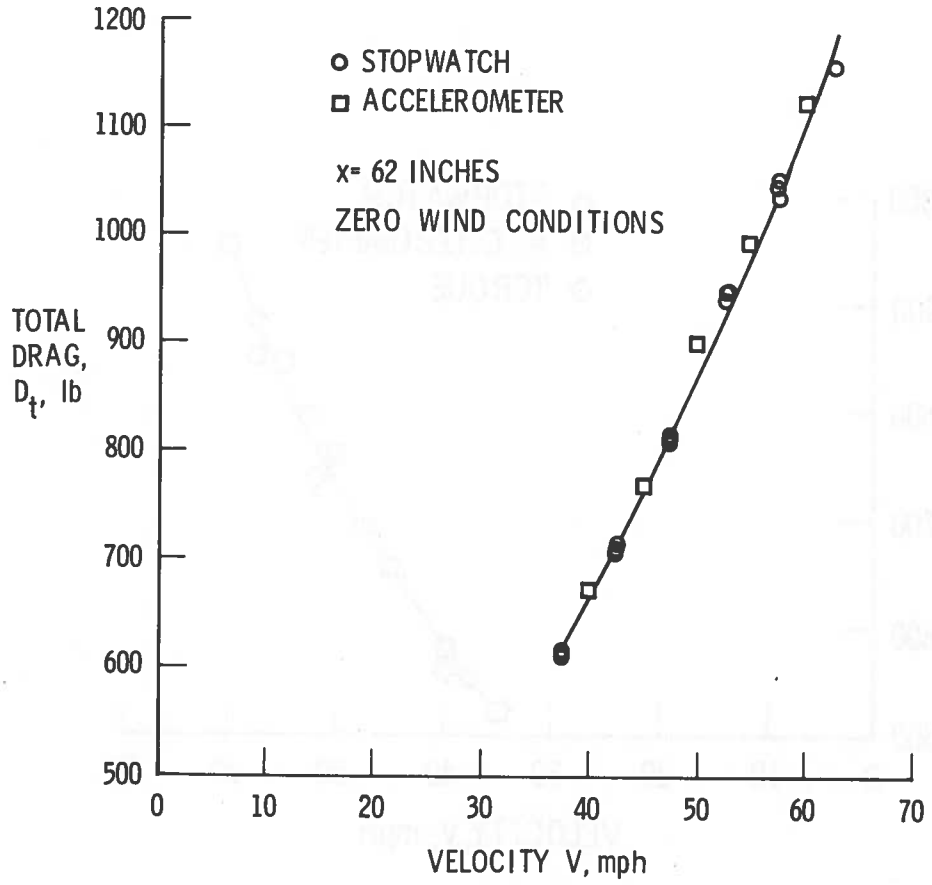

FIGURE 6. TYPICAL TOTAL DRAG FOR BASELINE CONFIGURATION

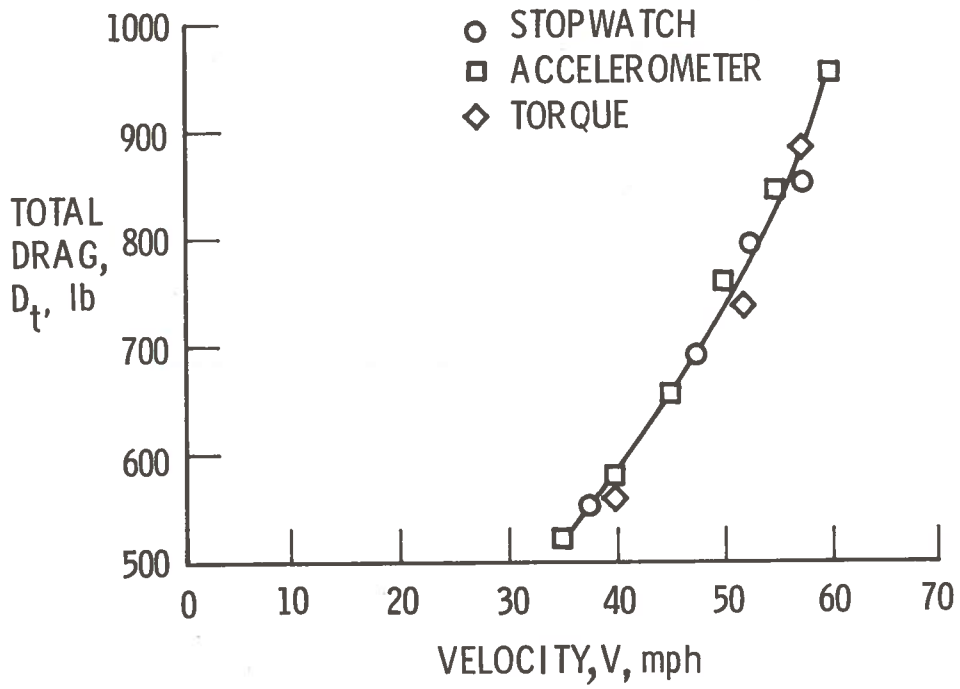

FIGURE 7. TOTAL DRAG OBTAINED FROM A TRACTOR-TRAILER COMBINATION USING THREE DIFFERENT METHODS

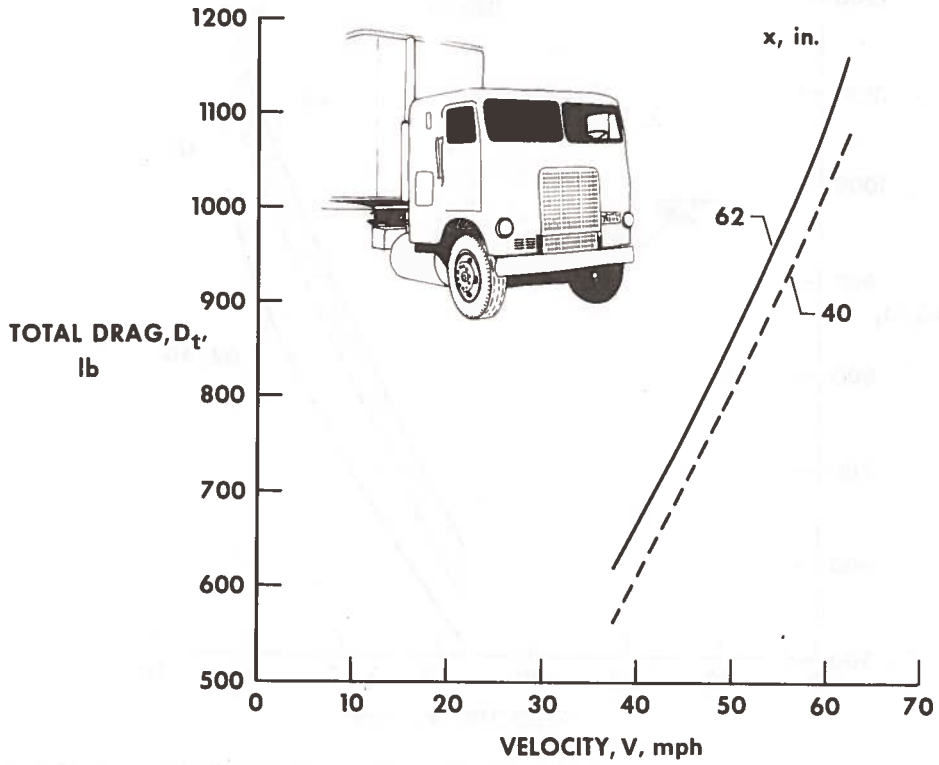

FIGURE 8. TOTAL DRAG FOR BASELINE CONFIGURATION FOR TWO TRAILER POSITIONS. ZERO WIND CONDITIONS

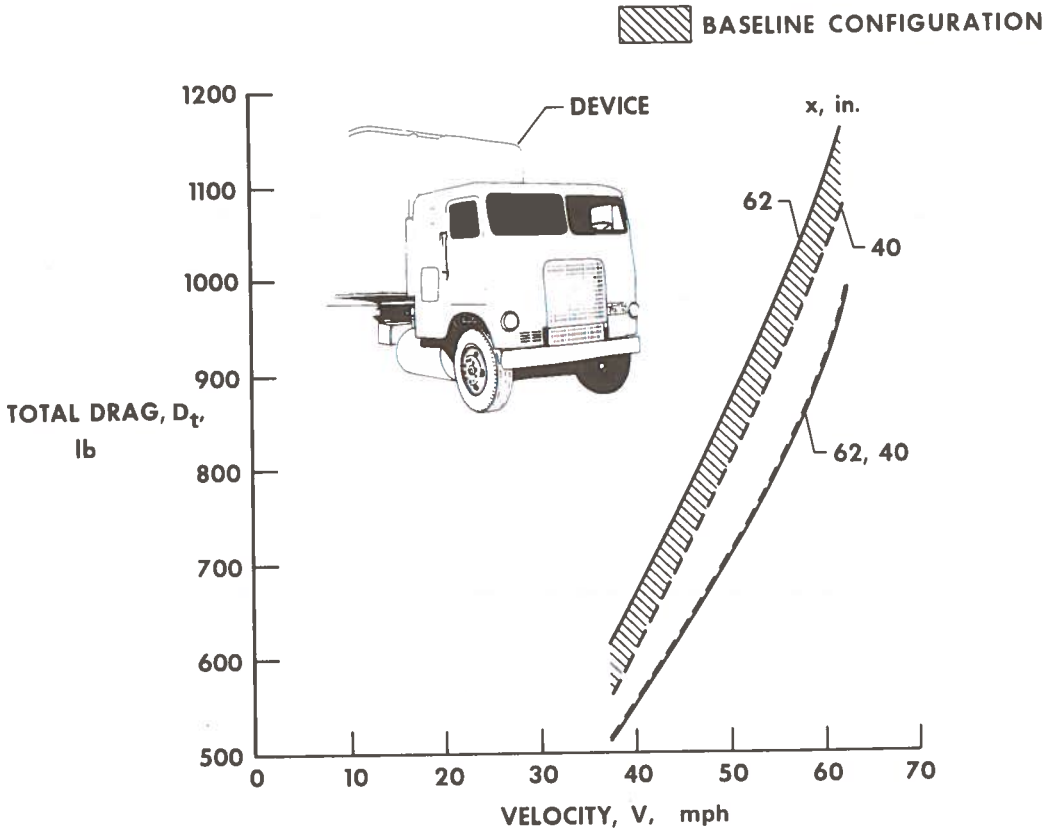

FIGURE 9. COMPARISON OF TOTAL DRAG WITH AND WITHOUT DEVICE A. ZERO WIND CONDITIONS

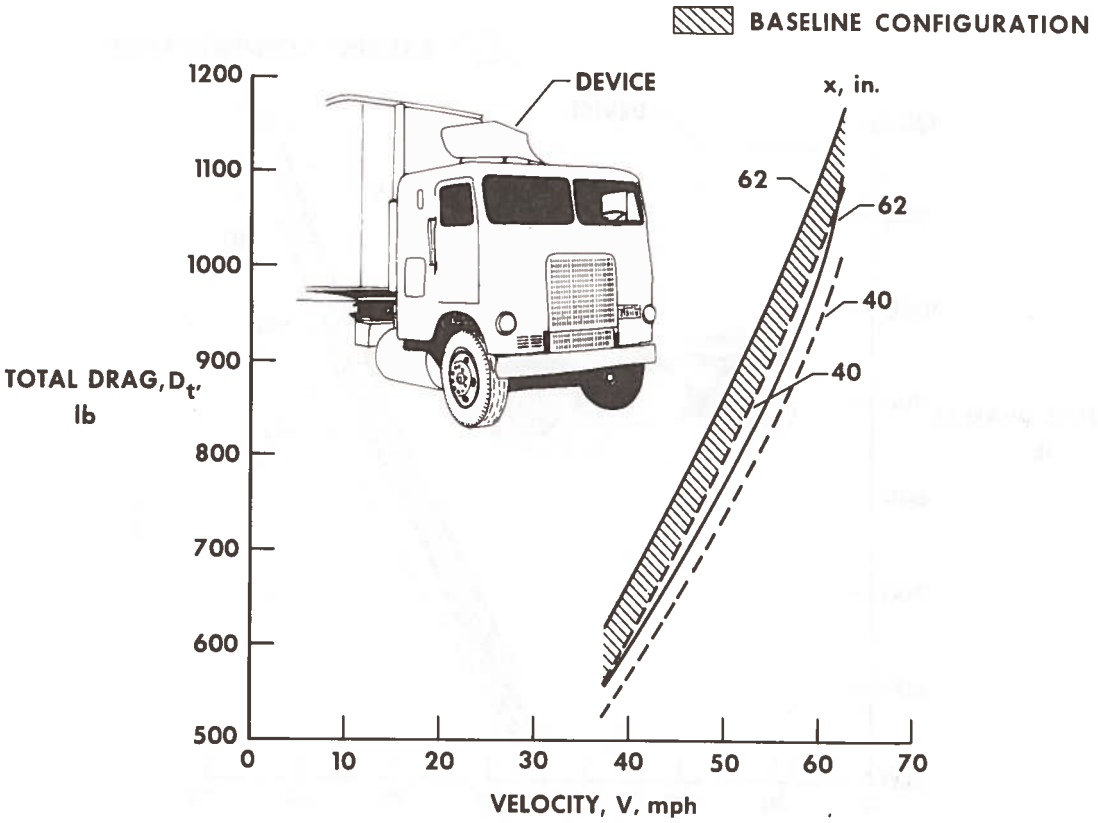

FIGURE 10. COMPARISON OF TOTAL DRAG WITH AND WITHOUT DEVICE B. ZERO WIND CONDITIONS

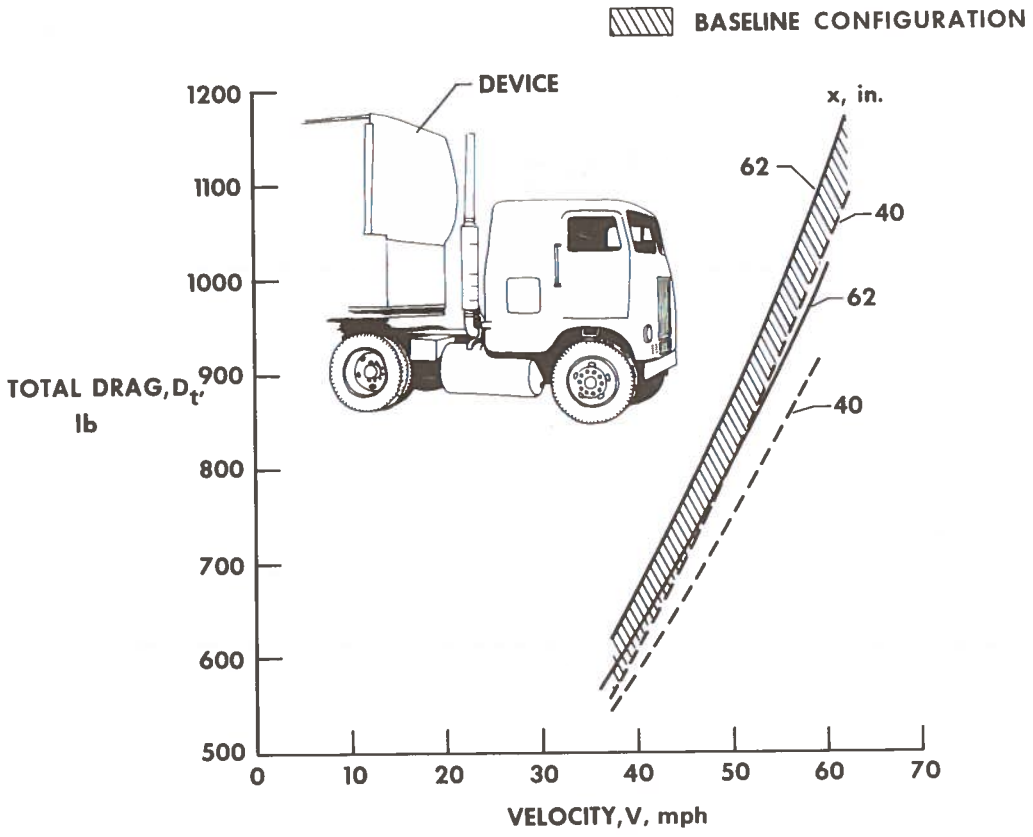

FIGURE 11. COMPARISON OF TOTAL DRAG WITH AND WITHOUT DEVICE C. ZERO WIND CONDITIONS

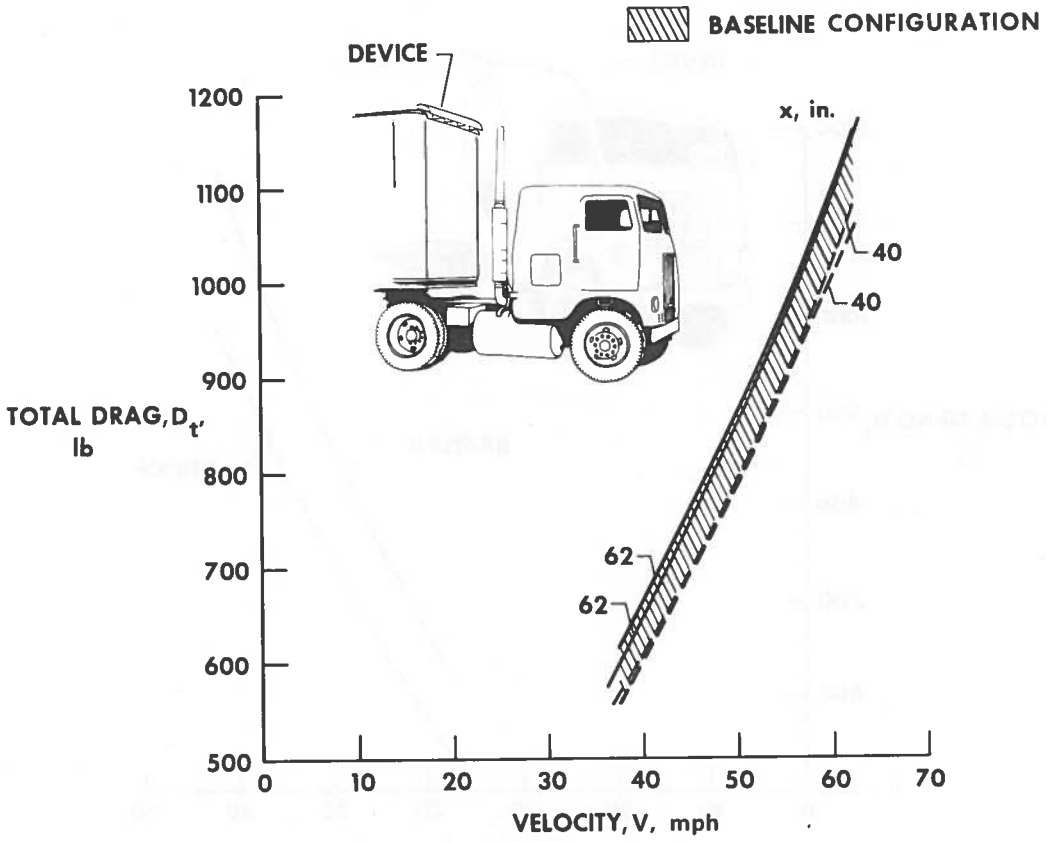

FIGURE 12. COMPARISON OF TOTAL DRAG WITH AND WITHOUT DEVICE D. ZERO WIND CONDITIONS

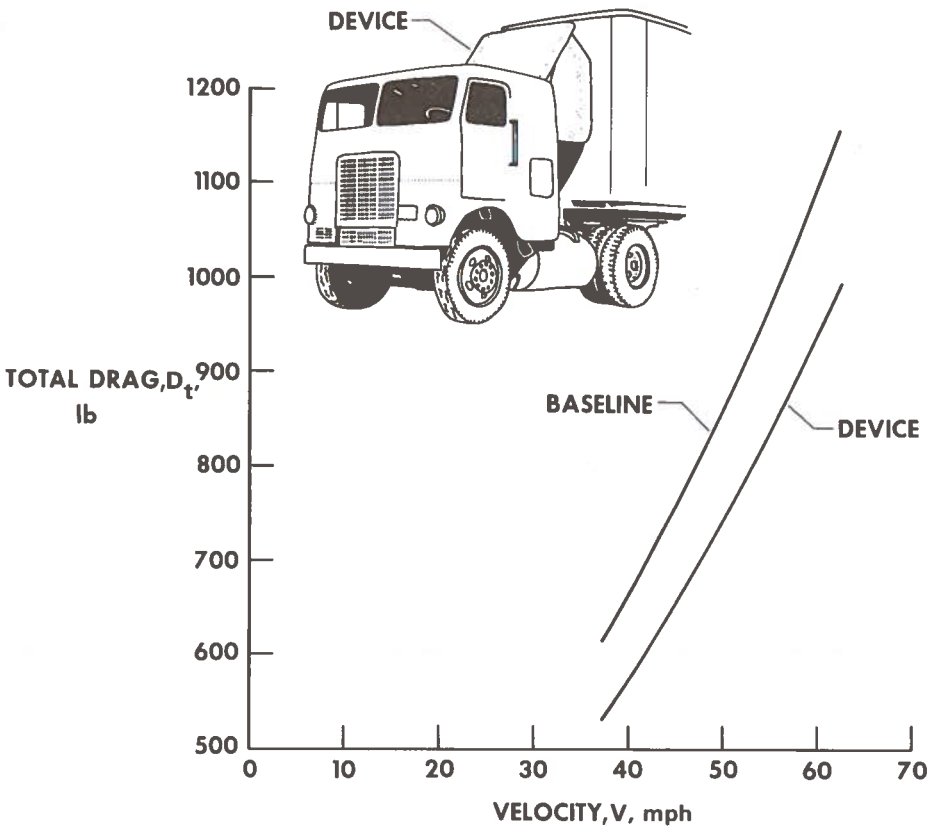

FIGURE 13. COMPARISON OF TOTAL DRAG WITH AND WITHOUT DEVICE E. ZERO WIND CONDITIONS

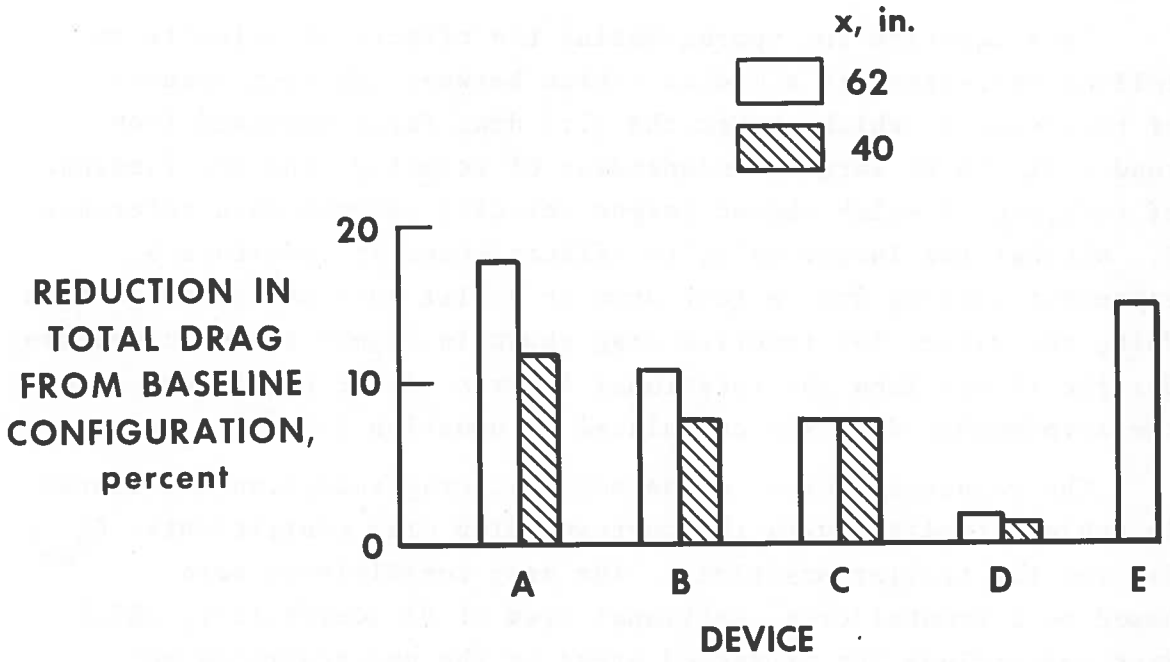

FIGURE 14. REDUCTION IN TOTAL DRAG FOR THE DEVICES. V=55 MILES PER HOUR, ZERO WIND CONDITIONS

As mentioned before, total drag consisted of aerodynamic plus mechanical drag. The tractive portion of the mechanical drag is shown in figure 15. The data point at approximately 1 mile per hour represents the value that was measured using two methods, the coast-down and tow methods, and the solid curve extrapolation is based on Hoerner's semiempirical equation for rolling resistance (ref. 7).

This equation for approximating the effects of velocity on rolling resistance is a median choice between the test results of reference 8, which showed the tire drag force obtained from road tests to be largely independent of velocity, and the findings of reference 9 which showed larger velocity effects than reference 7. Whether the larger velocity effects shown in reference 9 represent rolling over a test drum or a flat surface is not certain. Using the values for tractive drag shown in figure 15 and accounting for the thrust from the rotational inertia of the wheels and tires, the aerodynamic drag was calculated by equation (1).

The resulting values of aerodynamic drag reduction are listed in table 2 together with the corresponding drag coefficients, $C_{D_{ae}}$, for the two trailer positions. The drag coefficients were based on a frontal cross-sectional area of 94 square feet, which does not include the projected areas of the undercarriage and tires. The aerodynamic drag reduction ranged from 24 percent for device A for the rear trailer position to 2 percent for device D for the foward trailer position.

The drag coefficients (1.17 and 1.06) for the baseline configurations are higher than most sub-scale model results which have been reported for cab-over-engine tractor-trailer combinations (refs. 10 through 12). The radiator cover and reference area used in this study would account for higher calculated coefficients than reported in some instances. In addition, thus far the model data which have been available do not represent an adequate geometrical simulation of the subject full-scale vehicle. As stated in reference 4, there are other factors which can influence the value of aerodynamic drag coefficient which is calculated from

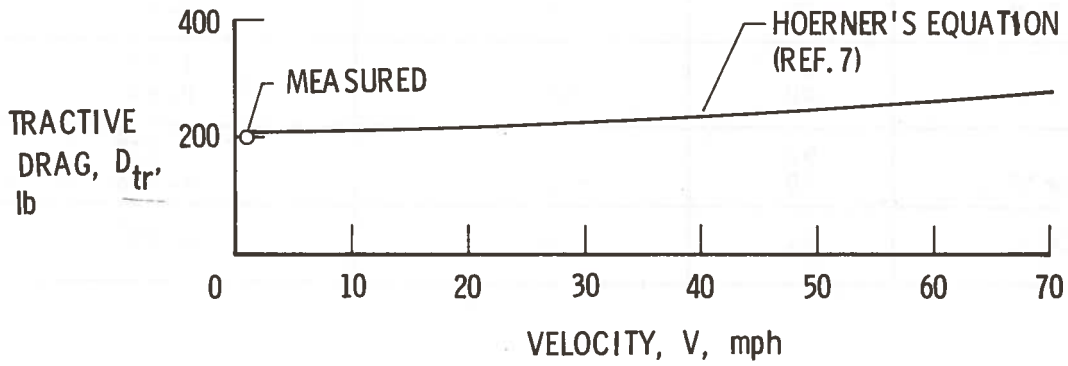

FIGURE 15. TRACTIVE DRAG

TABLE 2. AERODYNAMIC DRAG REDUCTION AND DRAG COEFFICIENTS

55 mpg, zero wind conditions			
Configuration	x, in.	Aerodynamic drag reduction, $\%\Delta D_{ae}$	Drag coefficient, $C_{D_{ae}}$
Baseline	62 40	-- --	1.17 1.06
Device A	62 40	-24 -16	0.89 0.89
Device B	62 40	-14 -11	1.00 0.94
Device C	62 40	-11 -11	1.04 0.94
Device D	62 40	- 3 - 2	1.13 1.04
Device E	62	-19	0.95

a set of data. Some of these factors are listed below.

1. Use of other approximations for the effects of velocity on tire rolling drag

2. Different reference area

3. Accounting for cooling drag (radiator was covered in these tests)

4. Use of approximation for the effects of velocity on coasting drive-line drag

Reference 8 presents two values of drive-line drag for application to coast-down data. There is a significant difference between these two sets of drive-line drag data (approximately a factor of two for a tandem axle-hypoid). The values from the main part of reference 8 were obtained from spin-down tests while the wheels of the test vehicle were jacked up clear of the road. It is not clear how the values presented in the accompanying discussion in reference 8 were obtained, but they approximate other unpublished values for a comparable drive line that was bench tested by measuring the power required to drive the system from the axle end of the system at constant rpm.

One would expect the gear loading conditions to be different for spin-down and constant-rpm tests. Perhaps this is the cause of the twofold differences noted above. In any event, it is believed that the gear loading for a given system during a coast-down test on a roadway would be uniquely dependent on the aerodynamic drag (which dictates the deceleration rate of the drive line) and different from either gear loading for the results shown in reference 8. Therefore, neither set of drive-line drag data from reference 8 is subtracted from the total drag values reported herein in calculating aerodynamic drag.

An approach that would theoretically account for the proper drive-line drag, bearing drag, tire drag, and rotary inertia effects during coast-down tests is the method used in reference 13 (see fig. 7 of ref. 13). Unfortunately, the requirement for ideally steady headwinds and tailwinds and a smooth, level, hard test

surface would be a very difficult combination of conditions to achieve.

Because of the manner in which items 1 to 4, listed above, were handled in this study, the resulting drag coefficients may be considered rather upper limit values, and consequently the aerodynamic reduction percentages presented may be considered somewhat conservative for all devices, A to E.

For those who want to apply adjustments to the present results for calculating aerodynamic drag coefficients, (such as would result from the preceding factors 1 through 4) the appropriate information is tabulated for the baseline configuration in table 3. Inclusion of table 3 will permit users of these data to make comparisons between these data and other results by substituting their choice of reference area or tractive drag (tire rolling, drive line, etc.).

Further experence will undoubtedly refine the definition of tractive drag for various types of drive lines under coast-down conditions. At that time the optimum factors necessary to better define aerodynamic drag may be applied with greater confidence.

8.3 EFFECT OF CROSSWINDS

The total drag data presented thus far are for zero wind conditions. Limited data were also obtained with crosswinds for the basic configuration and for some modified configurations. These data show that the drag of the configurations with add-on devices was sensitive to crosswinds, whereas the drag of the basic configuration exhibited a smaller change. Figure 16 presents the total drag results for a 2 to 3 mile-per-hour crosswind at an angle of approximately 11 degrees relative to the longitudinal axis of the vehicle for the basic configuration and devices A, B, and C. These results are for the rear trailer position (x = 62 inches) and represent the average of runs in two directions. Although the data do not define wind effects in detail, they indicate that in general the crosswinds reduced the ability of the add-on devices to decrease drag.

Figure 17 compares the total drag reduction obtained with three of the add-on devices with and without crosswinds for the rear

TABLE 3. BASELINE RESULTS IN COMPONENT FORM

Configuration	x,in.	D_{tr}, lb	R, lb	$C_{D_{ae}}$	D_t, lb
Baseline	62	252	58	1.17	977
Baseline	40	252	56	1.06	905

Where: V = 55 mph (no wind)
W = 32,000 lbs
A = 94 ft^2
q = 7.1 lb/ft^2
w = 8 ft.
h = 13.5 ft

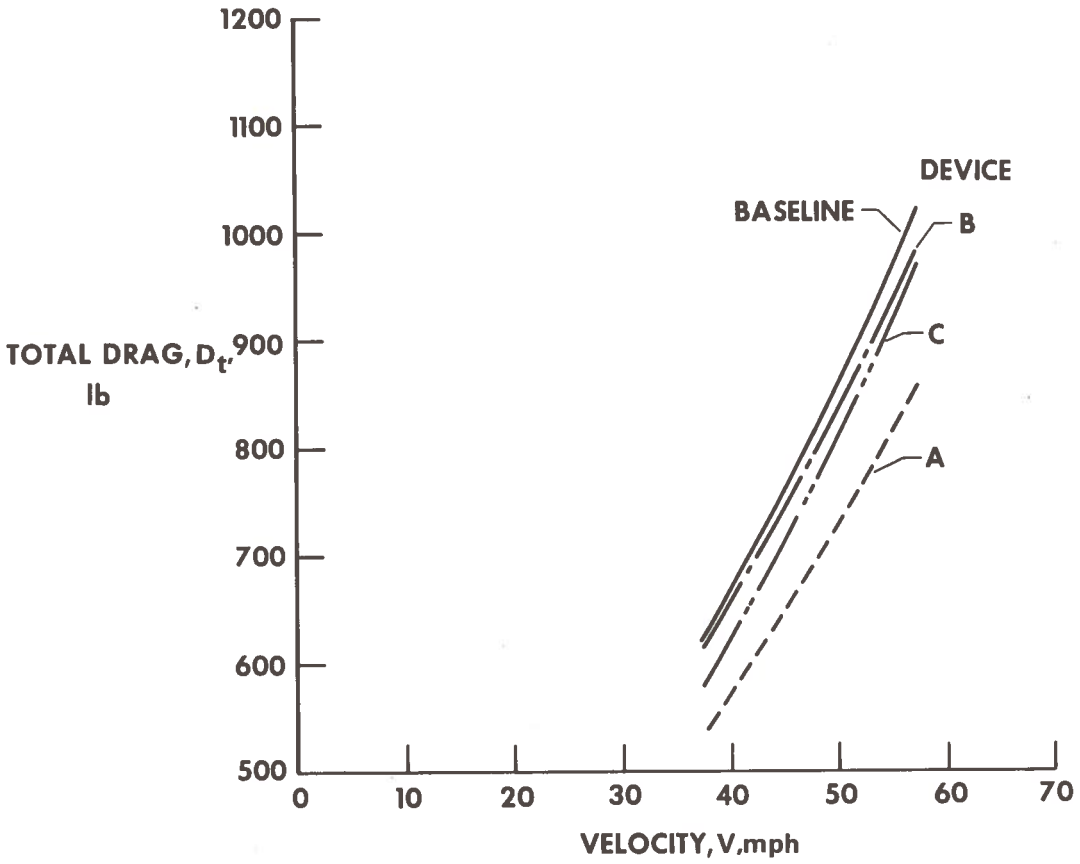

FIGURE 16. TOTAL DRAG WITH CROSSWINDS OF 2 TO 3 MILES PER HOUR AT AN ANGLE OF ABOUT 11°. x = 62 inches

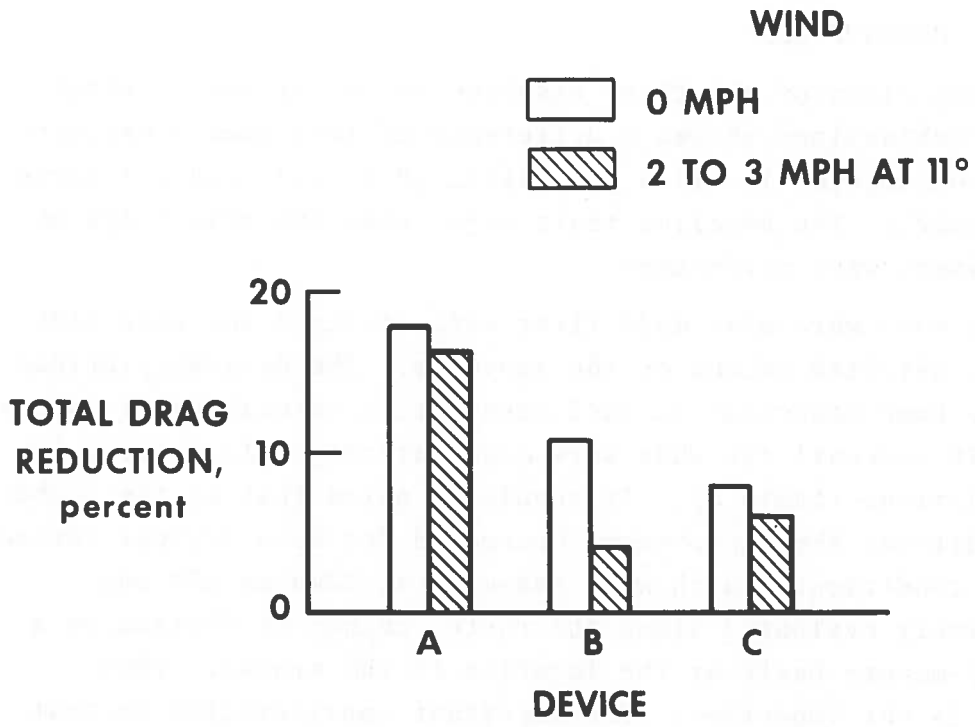

FIGURE 17. REDUCTION IN TOTAL DRAG FOR DEVICES A, B, AND C WITH AND WITHOUT CROSSWINDS. x = 62 INCHES, V = 55 MILES PER HOUR

trailer position. The data for the zero wind condition in figure 17 are the same as shown in figure 14. The total drag reduction decreased from 18 percent to 16 percent for device A, from 11 percent to 4 percent for device B, and from 8 percent to 6 percent for device C. These drag data obtained in crosswinds were limited and should be quantitatively substantiated by additional testing, however the detrimental influence of crosswinds is definitely established in a qualitative sense.

8.4 FUEL CONSUMPTION

A comparison of the three baseline tests for both tractor-trailer combinations showed a difference of less than 1 percent in fuel consumption in miles per gallon (0.8, 0.4, and 0.1 percent, respectively). The baseline tests were three 300-mile trips on which drivers were alternated.

Test runs were also made first with device A and then with device E installed on one of the vehicles. The devices provided about the same reduction in fuel consumption (a maximum of approximately 10 percent) for what were qualitatively calm-to-very-low wind conditions (table 4). It should be noted that at the higher wind conditions the improvement decreased for both devices tested. The wind conditions, which were measured at Edwards AFB and qualitatively evaluated along the route. cannot be defined on a minute-by-minute basis at the location of the trucks. This, however, is not important. The important consideration is that two trucks experienced the same load and rolling conditions, grades, traffic, and winds except for the displacement of position by about one-half mile at any given point in time. Furthermore, it should be realized that the relative wind direction, when there were winds, was wide ranging because the route was a closed loop. In spite of the variation of winds for different test days and different locations, the increments of fuel consumption shown in table 4 represent changes in aerodynamic drag of vehicles which experienced the same environment.

References 14 through 17 suggest that, at highway speeds, fuel savings, in percent, are between one third and one-half the

TABLE 4. FUEL ECONOMY TEST RESULTS FOR TWO DEVICES. V = 55 MILES PER HOUR

Source	Qualitative winds, mph	Fuel saving, percent	
		Device A	Device E
Prediction (refs. 14 to 17)	- - - -	8 to 12	6 to 9
Road test	0 to 5	10	- - -
	0 to 10	- - -	9.3
	0 to 15	- - -	7.7
	Up to 30	6.6	6
Road test	Up to 40	2.6	- - -

magnitude of the percentage of the reduction in aerodynamic drag. When this qualitative criterion is applied to the drag reductions measured for devices A and E, the resulting estimate of the maximum improvement in fuel consumption is as shown in the first line of table 4. It can be seen that the range of improvement suggested by references 14 through 17 is in general agreement with the fuel consumption improvement measured at the lower wind condition (0 to 15 mph).

8.5 FLOW VISUALIZATION

Flow visualization photographs were taken of the truck travelling at approximately 55 miles per hour (figs. 18 through 23). The airflow was made visible with a light colored powder (diatomaceous earth), which was emitted at the top front edge of the cab. The powder was pumped out of a sandblaster hopper inside the trailer under constant pressure. Although the photographs do not define the details of the stream tube paths, they provide visualization of the flow behavior with and without the add-on devices. It should be noted that the diatomaceous earth used in figures 18 and 22 produced a low density dispersion. The same general flow pattern resulted when diatomaceous earth that produced a high density dispersion was used. Crosswinds ranged from 2 to 5 miles per hour when the pictures were taken.

8.6 SIMULATION

Computer simulations were performed for a vehicle speed of 55 mph under assumed conditions of zero wind velocity. Results are summarized in table 5. As explained in the Method section of this report, the baseline configuration was considered to have an aerodynamic drag coefficient of 1.0. Four other cases were simulated, these having aerodynamic drag coefficients that were 20, 24, and 40 percent lower and 20 percent higher than the baseline case.

The baseline configuration has no entry in table 5 for percent change in $C_{D_{ae}}$ or percent change in fuel economy since results for other configurations are referenced to the baseline. The results predict that for the 32,500-lb vehicle the fuel economy ranges from

FIGURE 18. FLOW VISUALIZATION FOR BASELINE CONFIGURATION

FIGURE 19. FLOW VISUALIZATION FOR DEVICE A

FIGURE 20. FLOW VISUALIZATION FOR DEVICE B

FIGURE 21. FLOW VISUALIZATION FOR DEVICE C

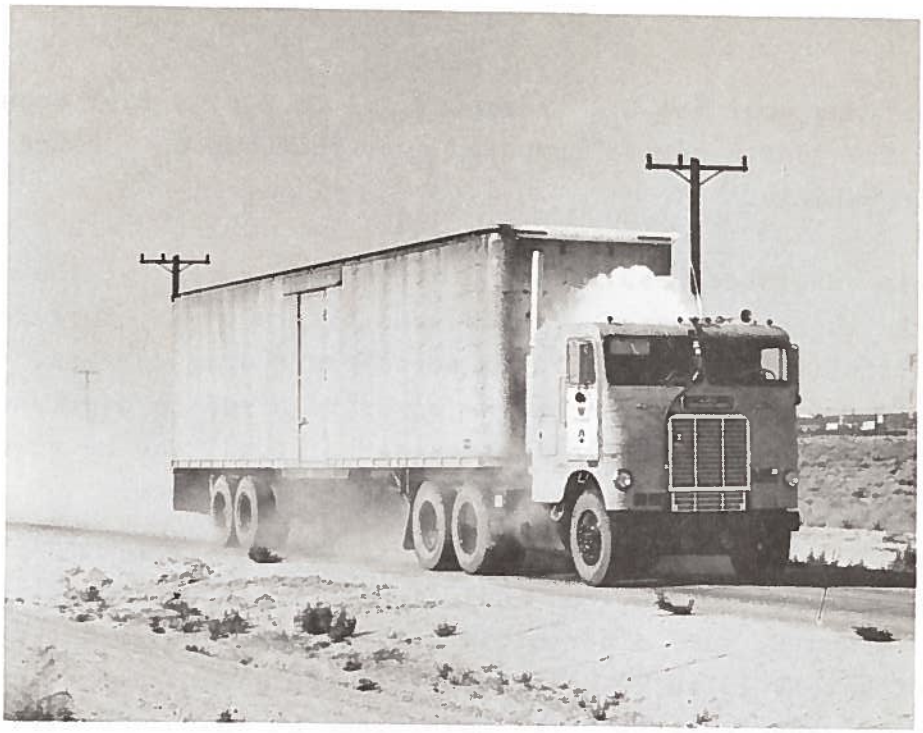

FIGURE 22. FLOW VISUALIZATION FOR DEVICE D

FIGURE 23. FLOW VISUALIZATION FOR DEVICE E

4.5 to 6.1 mpg over the $C_{D_{ae}}$ range of 1.2 to 0.6; a fuel economy range of 3.5 to 4.5 mpg is computed over the same $C_{D_{ae}}$ range for a 70,000-lb vehicle.

These tabulated results are plotted in figure 24. The curves illustrate the anticipated greater sensitivity of the fuel economy for a partially loaded vehicle to aerodynamic drag changes. With a fully loaded vehicle, the engine power required to overcome aerodynamic drag is a smaller percentage of total engine power output, primarily due to increased rolling resistance.

The coast-down tests of the full-scale vehicle fitted with add-on drag-reduction devices indicate the two most effective devices, A and E, have a potential of reducing aerodynamic drag by approximately 19 to 24 percent. Road tests for fuel economy of the same vehicles with speed maintained at approximately 55 mph show a fuel savings of about 9 to 10 percent, with wind conditions ranging qualitatively from zero to gusts of 10 mph. The predictions from the simulations with zero winds indicate a fuel economy savings in the range of 11 to 14 percent, which is in reasonable agreement with the results of the road tests.

TABLE 5. RESULTS OF VEHICLE SIMULATION. V = 55 MILES PER HOUR, ZERO WIND CONDITIONS

Vehicle Weight, W, lb	Quantity	Aerodynamic Drag Coefficient, $C_{D_{ae}}$				
		0.6	0.76	0.8	*1.0	1.2
	$\%\Delta C_{D_{ae}}$	-40	-24	-20	---	20
32,500	mpg	6.09	5.54	5.41	4.88	4.47
	%Δmpg	24.8	13.5	10.9	---	-8.4
70,000	mpg	4.53	4.20	4.13	3.79	3.50
	%Δmpg	19.5	10.8	9.0	---	-7.7

*Baseline

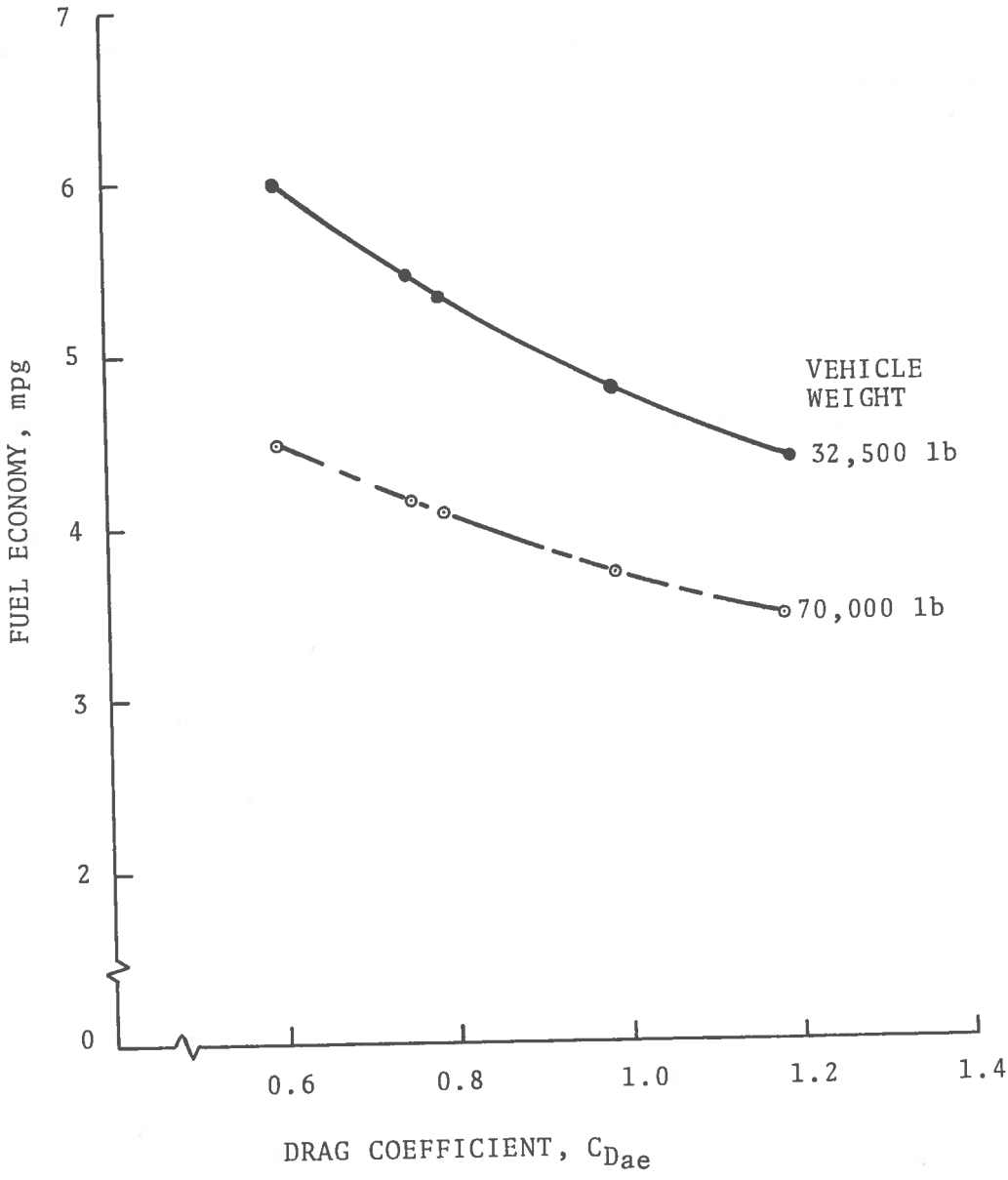

FIGURE 24. SIMULATED FUEL ECONOMY AS A FUNCTION OF AERODYNAMIC DRAG FOR A VEHICLE SPEED OF 55 MPH WITH NO WIND

9. CONCLUSIONS

The major conclusions derived from the foregoing study are listed below:

1. The maximum fuel savings realized were about 10 percent for devices A and E when exposed to calm or near calm wind conditions.

2. The maximum aerodynamic drag reduction realized with an add-on device at zero wind conditions was approximately 24 percent for the rear trailer position (cab-to-trailer gap of 62 in.). Some add-on devices provided only small reductions in drag.

3. Limited coast-down data obtained for some of the devices showed that their ability to decrease drag was reduced by the presence of crosswinds. This trend was confirmed in a qualitative sense by results from fuel consumption tests which were made during windy conditions.

4. Simulation of aerodynamic drag reductions of 20 to 24 percent produced fuel consumption reduction of 10.9 to 13.5 percent, respectively, for a 32,500-lb vehicle. Simulation of a fully loaded 70,000-lb vehicle for the same drag reductions showed fuel consumption reductions ranging from 9.0 to 10.8 percent.

5. Reducing the cab-to-trailer gap distance from 62 inches to 40 inches decreased the aerodynamic drag of the baseline configuration approximately 10 percent at zero wind conditions which corresponds to a total drag reduction of about 7 percent.

10. RECOMMENDATIONS

Tests of a similar nature to the study presented herein should be conducted to evaluate add-on devices with a conventional (long nose) tractor-trailer combination. In the event such tests are conducted it is recommended that the add-on devices evaluated include at least the two most successful, as determined in the present study.

The effects of crosswinds are also an area of major importance and a systematic research effort is needed. Wind-tunnel studies are probably the most promising approach to an adequate understanding of cross-winds effects; however there may be a need for some full-scale real vehicle experiments following the wind tunnel tests.

APPENDIX

LIST OF MANUFACTURERS OF DEVICES TESTED

Device	Description	Manufacturer
A	"AIRSHIELD®"	Rudkin-Wiley Corp. 760 Honeyspot Rd. Stratford CT 06497
B	"AIRFLO"	Airflow Co. P. O. Box 705 Elkhart IN 46514
C	"NOSE CONE"	Nose Cone Manufacturing Co. 9331 Mikinda Ave. La Habra CA 90631
D	"AIRVANE"	Systems. Science and Software P. O. Box 1620 La Jolla CA 92037
E	"AEROVANE"	Aero Van Inc. 4074 Ridge Rd. Smyrna GA 30080

REFERENCES

1. Edwin J. Saltzman and Robert R. Meyer, Jr., "Drag Reduction Obtained by Rounding Vertical Corners on a Box-Shaped Ground Vehicle." NASA TM X-56023, 1974.

2. Edwin J. Saltzman, Robert R. Meyer, Jr., and David P. Lux, "Drag Reductions Obtained by Modifying a Box-Shaped Ground Vehicle." NASA TM X-56027, 1974.

3. Lawrence C. Montoya and Louis L. Steers, "Aerodynamic Drag Reduction Tests on a Full-Scale Tractor-Trailer Combination with Several Add-On Devices." NASA TM X-56028, 1974.

4. Louis L. Steers, Lawrence C. Montoya, and Edwin J. Saltzman, "Aerodynamic Drag Reduction Tests on a Full-Scale Tractor-Trailer Combination and a Representative Box-Shaped Ground Vehicle." SAE 750703, 1975

5. R. A. White and H. H. Korst, "The Determination of Vehicle Drag Contributions from Coast-Down Tests." SAE 720099, 1972.

6. A. C. Malliaris, E. Withjack, and H. Gould, "Simulated Sensitivities of Auto Fuel Economy, Performance and Emissions." SAE 760157, Feb. 1976.

7. Sighard F. Hoerner, "Fluid-Dynamic Drag" Publ. by the author (P.O. Box 342, Bricktown NJ 08723) 1965.

8. J. W. Anderson, J. C. Firey, P. W. Ford, and W. C. Kieling, "Truck Drag Components by Road Test Measurement." and accompanying discussion, S.A.E. Transactions 1965, Vol. 73, 1965, pp. 148-159.

9. J. A. Davisson, "Design and Application of Commercial Type Tires." SAE SP-344, Jan. 1969.

10. Harold Flynn and Peter Kyropoulos, "Truck Aerodynamics." SAE Transactions 1962, Vol. 70, c. 1962, pp. 297-308.

11. A. Wiley Sherwood, "Wind Tunnel Test and Trailmobile Trailers." Wind Tunnel Rep. No 85 Univ. Maryland, June 1953.

12. "Proceedings of the Conference/Workshop on Reduction of the Aerodynamic Drag of Trucks," Oct. 10-11, 1974. (Available from Nat. Sci. Foundation RANN Document Center, 1800 "G" St., N. W., Washington DC 20550.)

13. Peter B. S. Lissaman and Jack H. Lambie, "Reduction of Aerodynamic Drag of Large Highway Trucks." Proceedings of the Conference/Workshop on Reduction of the Aerodynamic Drag of Trucks, Oct. 10-11, 1974, pp. 139-151. (Available from Nat. Sci. Foundation RANN Document Center, 1800 "G" St., N. W., Washington DC 20550.)

14. H. Schlichting, "Aerodynamic Problems of Motor Cars." AGARD Rep. 307, Oct. 1960.

15. Dave Ritchie, "How to Beat the Built-In Headwind." Owner Operator, May-June 1973, pp. 89-99.

16. Carl E. Burke, Larry H. Nagler, E. C. Campbell, W. E. Zierer, H. L. Welch, L. C. Lundstrom, T. D. Kosier, and W. A. McConnell, "Where Does All the Power Go?" SAE Transactions, Vol. 65, 1957, pp. 713-738.

17. Thomas C. Austin and Karl H. Hellman, "Passenger Car Fuel Economy - Trends and Influencing Factors." SAE 730790, 1973.